MICROSTRUCTURAL CHARACTERIZATION OF FeNi ALLOYING IN ALUMINIUM BASED ALLOYS

Widi S. Raharjo[1)] and Eddy A. Basuki[2)]

[1)] Undegraduate student, and [2)] Associate Professor

Department of Metallurgical Engineering
Faculty of Mining and Petroleum Engineering
Bandung Institute of Technology
www.metallurgy.itb.ac.id

Abstract

Most of metallic elements have alloying capability with aluminium and only few are important major alloying ingredients in commercial aluminium based alloys. Nevertheless, an appreciable number of other elements, such as Fe and Ni, serve as supplementary alloying additions for improving alloy properties especially wear resistance and high temperature strength. The role of element additions in aluminium alloys are normally contribute in one of two different strengthening mechanisms i.e., precipitation strengthening for elements like Cu, Mg, Mn and Zn that give ageing effect, and dispersion strengthening for elements of Si, Fe and Ni that produce dispersion of either elemental or intermetallic phase particles in aluminium matrix. The mechanical properties of these alloys are strongly depends on the microstructures of the alloys. This paper reports the results of microstructural characterization of aluminium alloys as results of FeNi alloying.

Keywords: Aluminium alloys, Al-Fe-Ni alloys, intermetallic phase, microstructural characterization

I. INTRODUCTION

The unique combinations of properties provided by aluminium alloys make these alloys one of the most versatile, economical and attractive metallic materials for broad range of uses, from very soft and highly ductile wrapping foil to the most relatively strong and hard of demanding engineering applications. It has been recognized that aluminium alloys are the second after steels in use as structural metals[(1)].

The predominant reason for alloying in aluminium alloys is to increase strength, hardness and resistance to wear, creep, stress relaxation or fatigue[(2)]. Effects on these properties are specific to the different alloying elements and combinations of them, and are related to their alloy phase diagram and to the microstructures and substructures that they form as a result of solidification or casting, thermomechanical history, heat treatment and/or cold working.

The elements that are most commonly present in commercial alloys to provide increase strength particularly when couple with strain hardening by cold working or with heat treatment, or both – are copper, magnesium, tin, manganese, silicon, and zinc. These elements, except silicon, all have significant solid solubility in aluminium, and in all cases the solubility increases with increasing temperature, and therefore are recognized as heat-treatable alloys[1,2].

Nickel improves the strength and hardness of cast and wrought aluminium-copper-magnesium alloys at elevated temperature. The solid solubility of nickel in aluminium is limited at 0.04%. Over this amount, it is present as an hard insoluble intermetallic, such as Al_3Ni, usually in combination with iron as $Al_3(Ni,Fe)$[4]. Nickel is added to wrought alloys 2018, 2218 and 2618, which were developed for elevated temperature service, and to certain 3xxx cast alloys used for pistons, cylinder blocks, and other engine parts subjected to high temperatures[5].

Iron has high solubility in molten aluminium, but its solubility in the solid state is only 0.05%, and therefore, similar to that occur in alloying with nickel, most of the iron present in aluminium appears as hard intermetallic second phases in combination with aluminium, such as Al_6Fe and Al_3Fe. Iron and nickel reduce the grain size of most aluminium alloys that give useful combinations of strength and ductility at room temperature and retain strength at elevated temperatures. The properties are due to the fine grain size that is stabilized by the finely dispersed hard iron-nickel rich second phase.

The microstructural characteristics when ferro-nickel is introduced into relatively pure aluminium are investigated in this study using optical and electron microscopes. The ferro-nickel was the low-carbon FeNi shots of PT. Aneka Tambang Pomalaa smelter, while the high purity aluminium ingot was obtained from PT. Inalum. The results of this study are used for the basic knowledge for further microstructural improvement of the aluminium alloys dedicated for high temperature applications of moving parts in automotive engines. An appreciable number of ternary Al-Fe-Ni phase diagrams[6,7,8,9,10] were utilized to confirm the reactions or phase transformations that might occur for the formation of microstructures of the ternary aluminium alloys.

II. EXPERIMENTAL

The nominal chemical composition of 6 (six) alloys for this study are shown in Table 1 (al compositions are in weight percent unless stated otherwise). These chemical compositions o the alloys can be ploted on the ternary phase diagram of Al-Fe-Ni at 600°C as shown ir Figure 1. The alloys were produced by melting the aluminium in an electric furnace at 750°C and addition of FeNi in the molten aluminium for about 10 minutes. The chemical compositior of the FeNi alloying elements is approximately 76.6Fe-22.7Ni-0.3Co-0.01C-0.1Si-0.1Cr. Afte air cooling to room temperature, the alloys were cut into several coupon samples having approximate dimension (in mm) of 10 x 15 x 15. Prior to optical and electron microscopy, the samples were mounted in an epoxy resin and polished to a 1 µm finish, and ther ultrasonically cleaned in acetone.

To reveal the microstructures of the samples, the polished samples were etched in Kellen's reagents solution for about 10 seconds. Microstructural observations were initially carried ou on the etched samples using an optical microscope. Phase identification, either the matrixes or particles, based on the chemical compositions, was performed by energy dispersive x-ray analysis (EDAX) facility attached in an scanning electron microscope. Microhardness testing was performed on the samples to measure the hardness of the average hardness values o the alloys. The average hardness value of each sample was obtained from 20 individua hardness tests performed on the random places of the surface sample.

Table 1
Chemical composition of alloy samples

Alloy	*Al (wt%)*	*Fe (wt%)*	*Ni (wt%)*
1	96.72	2.35	0.93
2	96.41	1.34	2.25
3	96.03	0.31	3.66
4	98.23	1.29	0.48
5	98.17	0.69	1.14
6	98.01	0.18	1.81

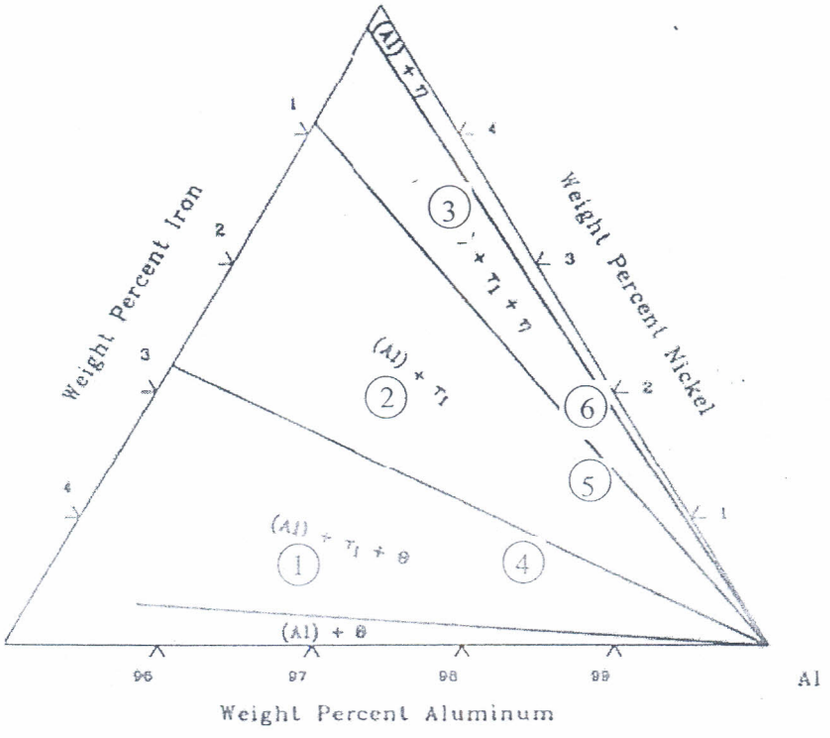

Figure 1. Phase diagram of ternary Al-Fe-Ni isothermal at 600^{0}C

III. RESULTS AND DISCUSSION

The microstructure of the alloy samples with different chemical compositions taken under optical and electron microscopes at various magnifications are shown in Figures 2 – 7. The figures clearly show that most of the alloys have dendritic structure, except alloy 5 that indicates peritectic structure. Figures 8 – 10 show the examples of some phase identifications of the alloys using EDAX. The alloy of (98.23Al-1.29Fe-0.48Ni) has second phase Al_3Fe intermetallic particles dispersed mostly along the interdendritic regions, as shown in Figure 2.

In addition to Al_3Fe, other intermetallic phases, Al_3Ni and Al_9FeNi, also occur in alloy of (98.17Al-0.69Fe-1.14Ni), as indicated at Figure 3; while alloy (98.01Al-0.18Fe-1.81Ni) only has single Al_3Ni particle (Figure 4). Increasing the content of Al_9FeNi particles were found in the alloys of (96.72Al-2.35Fe-0.93Ni), (96.41Al-1.34Fe-2.25Ni) and (96.03Al-0.31Fe- 3.66Ni), as shown in Figures 5, 6 and 7.

It is important to note that Al_9FeNi or τ_1 phase is formed at 809°C[9] through the following peritectic reaction : $L + Fe_4Al_{13} + NiAl_3 \leftrightarrow \tau_1$. At lower temperature, i.e., 620°C, the phase of Al_9FeNi has chemical composition of Fe and Ni in the range of 4.42 to 11.11 at.% and 7.01 to 13.5 at.% for Fe and Ni respectively. This peritectic reaction is shown at Figure 12 by point P_3. In addition to this peritectic reaction that produce τ_1 phase, an eutectic reaction of $L \leftrightarrow (Al) + \tau_1 + NiAl_3$ can occur at 638°C[10] as indicated by point E2 at Figure 11, and an eutectoid reaction of $L + Fe_4Al_{13} \leftrightarrow (Al) + \tau_1$ should also occur at 650°C[10] as indicated by point U_2 at Figure 11.

Therefore, it is concluded that τ_1 phase that occurred in the alloy samples from these three reactions at several different temperatures. The consequence of these different intermetallic phase particles in the alloys is that their mechanical properties that measured by the microhardness varies as indicated by the results of microhardness measurement shown in Table 2. The alloy 4 (98.23Al-1.29Fe-0.48Ni) has higher hardness compared to alloy 6 (98.01Al-0.18Fe-1.81Ni) as alloy 4 (98.23Al-1.29Fe-0.48Ni) produce Al_3Fe while Al_3Ni was found in alloy 6 (98.01Al-0.18Fe-1.81Ni) and this is confirmed by the phase diagrams shown in Figure 11 and 12. The Alloy 1 (96.72Al-2.35Fe-0.93Ni), 2 (96.41Al-1.34Fe-2.25Ni), 3 (96.03Al-0.31Fe- 3.66Ni) and 5 (98.17Al-0.69Fe-1.14Ni) had the mixture of phases of Al_3Fe, Al_3Ni and Al_9FeNi that make these alloy increase their hardness.

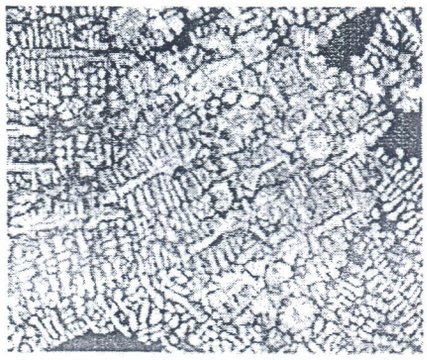

(a) 50μm

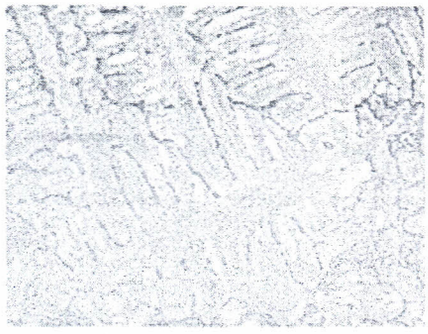

(b) 10μm

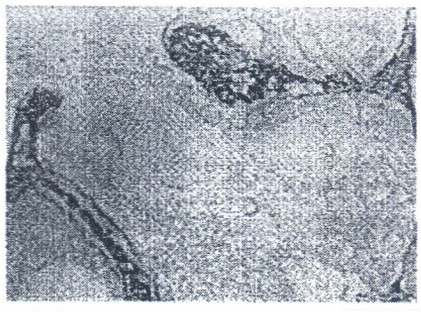

(c) 2μm

(d) 10μm

Figure 2. Microstructure of 98.23Al 1.29Fe 0.48Ni alloy (4) (a) taken under optical microscope at 50x, (b) 200x and (c) at 1000x, (d) taken under electron microscope at 2000x.

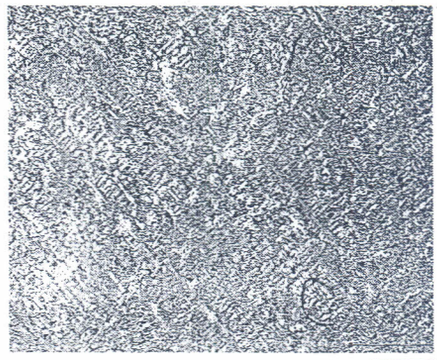

(a) 50μm

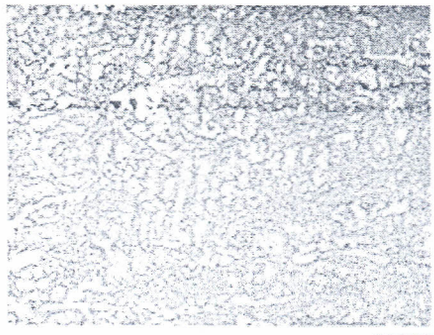

(b) 10μm

(c) 2μm

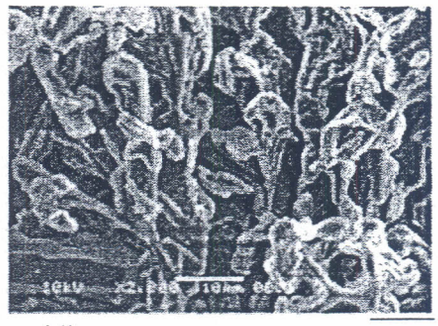

(d) 10μm

Figure 3. Microstructure of 98.17Al 0.69Fe 1.14Ni alloy (5) (a) taken under optical microscope at 50x, (b) 200x and (c) at 1000x, (d) taken under electron microscope at 2000x.

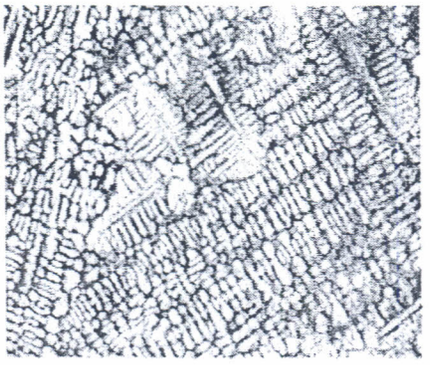

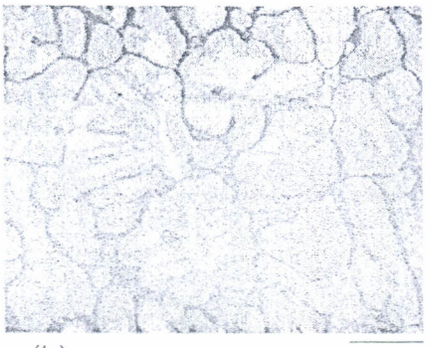

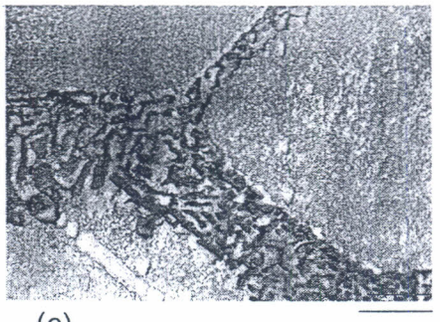

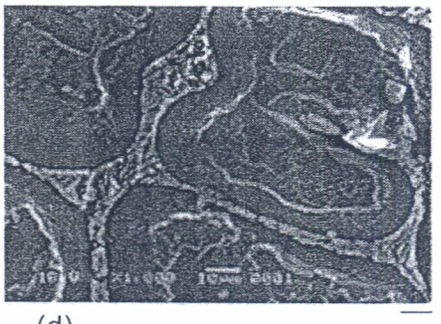

Figure 4. Microstructure of 98.01Al 0.18Fe 1.81Ni alloy (6) (a) taken under optical microscope at 50x, (b) 200x and (c) at 1000x. (d) taken under electron microscope at 1000x

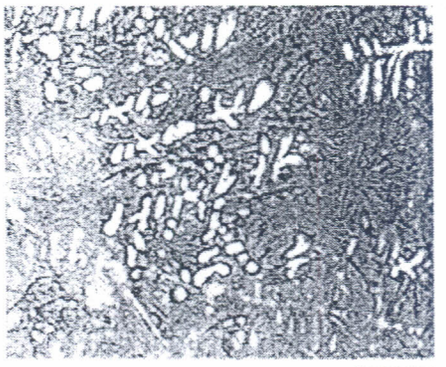

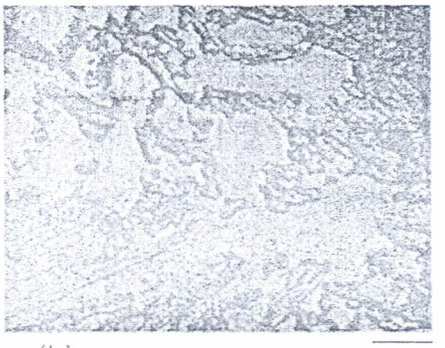

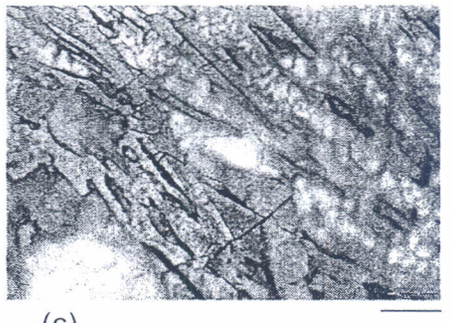

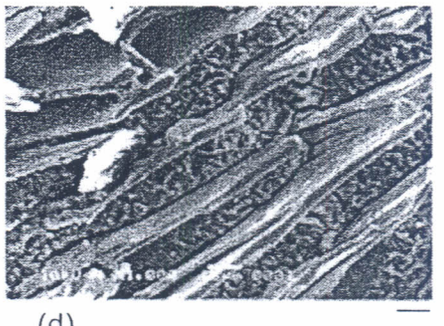

Figure 5. Microstructure of 96.72Al 2.35Fe 0.93Ni.alloy (1) (a) taken under optical microscope at 50x, (b) 200x and (c) at 1000x. (d) taken under electron microscope at 1000x

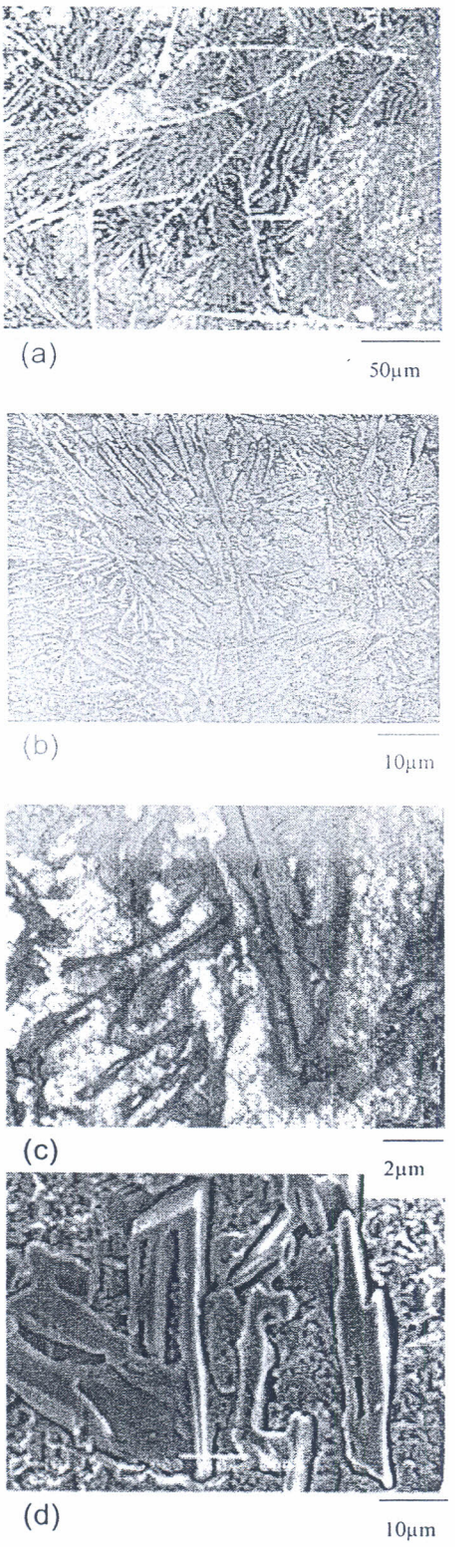

Figure 6. Microstructure of 96.41Al 1.34Fe 2.25Ni alloy (2) (a) taken under optical microscope at 50x, (b) 200x and (c) at 1000x. (d) taken under electron microscope at 2000x

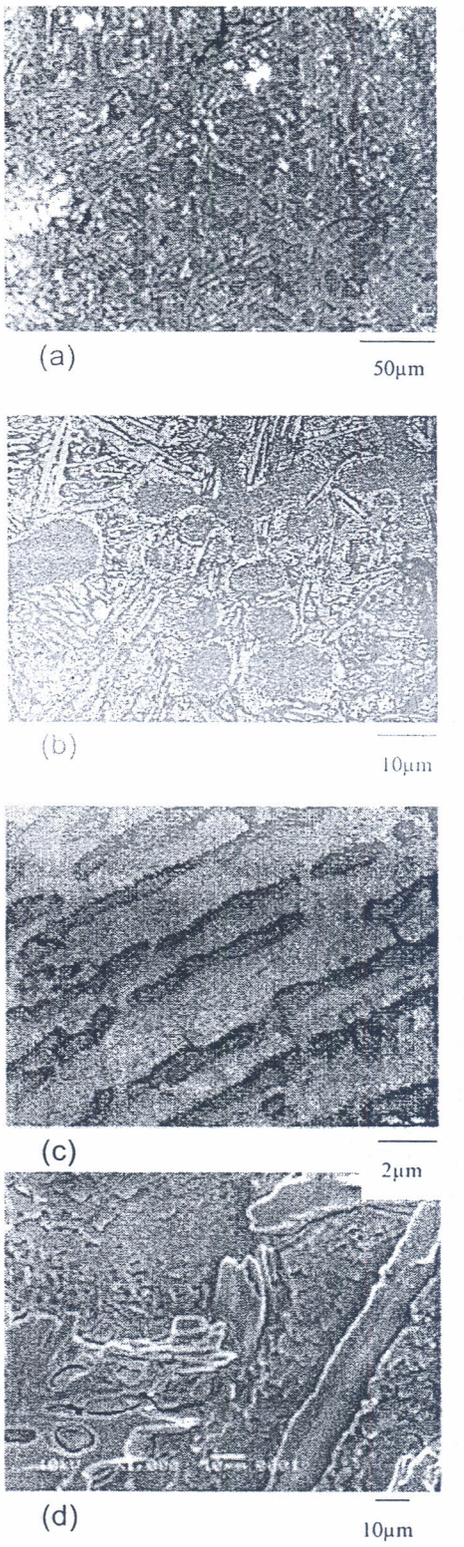

Figure 7. Microstructure of 96.03 Al 0.31 Fe 3.66Ni alloy (3) (a) taken under optical microscope at 50x, (b) 200x and (c) at 1000x. (d) taken under electron microscope at 2000x

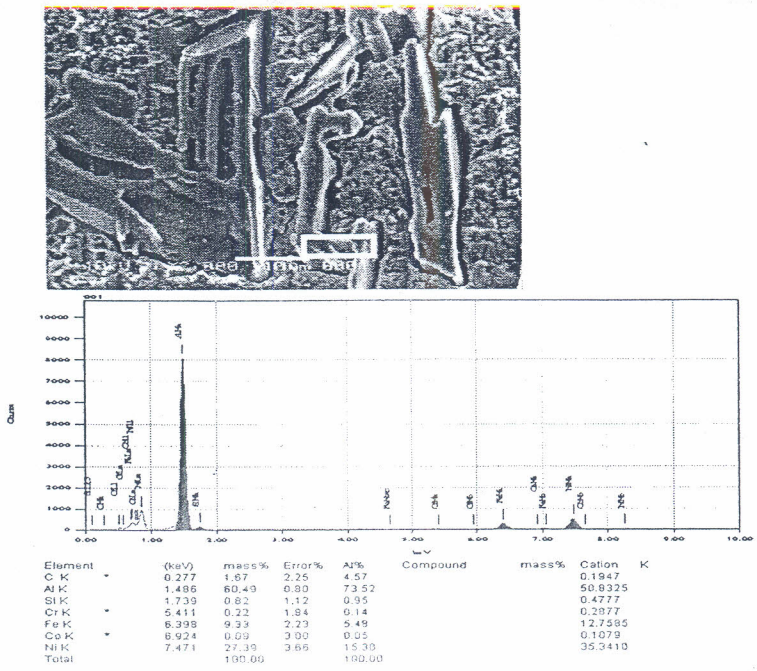

Element		(keV)	mass%	Error%	At%	Compound	mass%	Cation	K
C K	*	0.277	1.67	2.25	4.57			0.1947	
Al K		1.486	60.49	0.80	73.52			50.8325	
Si K		1.739	0.82	1.12	0.95			0.4777	
Cr K	*	5.411	0.22	1.84	0.14			0.2877	
Fe K		6.398	9.33	2.23	5.49			12.7585	
Co K	*	6.924	0.09	3.00	0.05			0.1079	
Ni K		7.471	27.39	3.66	15.30			35.3410	
Total			100.00		100.00				

Figure 8. Identification of Al_9FeNi or τ_1 phase (Co_2Al_9-type monoclinic)

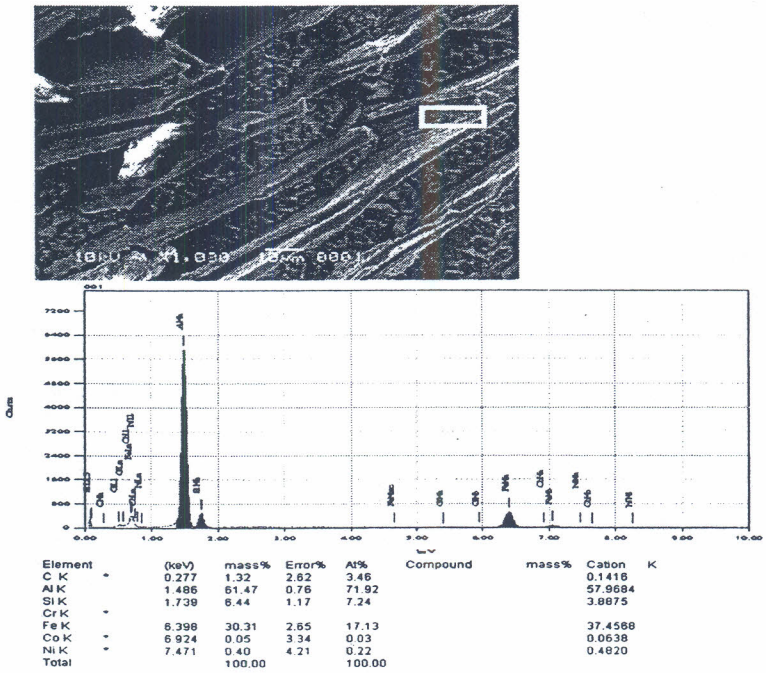

Element		(keV)	mass%	Error%	At%	Compound	mass%	Cation	K
C K	*	0.277	1.32	2.62	3.46			0.1416	
Al K		1.486	61.47	0.76	71.92			57.9684	
Si K		1.739	6.44	1.17	7.24			3.8875	
Cr K	*								
Fe K		6.398	30.31	2.65	17.13			37.4568	
Co K	*	6.924	0.05	3.34	0.03			0.0638	
Ni K	*	7.471	0.40	4.21	0.22			0.4820	
Total			100.00		100.00				

Figure 9. Identification of Al_3Fe or Fe_4Al_{13} phase (monoclinic type)